Available online at www.sciencedirect.com
SCIENCE DIRECT
Journal of Chromatography B, 826 (2005) 91–107
JOURNAL OF CHROMATOGRAPHY B
www.elsevier.com/locate/chromb

N-terminal isotope tagging with propionic anhydride: Proteomic analysis of myogenic differentiation of C2C12 cells

Hyung Wook Nam [a], Richard Simpson [b], Yu Sam Kim [a,*]

[a] *Department of Biochemistry, College of Science, Protein Network Research Center, Yonsei University, 134 Sinchon-dong, Seoul 120-749, Republic of Korea*
[b] *Joint ProteomicS Laboratory (JPSL), Ludwig Institute for Cancer Research, Walter and Eliza Hall Institute of Medical Research, Melbourne, Vic., Australia*

Received 14 March 2005; accepted 10 July 2005
Available online 13 September 2005

Abstract

N-Terminal isotope tagging (NIT) is an important proteomic tool for quantifying proteins in complex mixtures. Here we describe a modified version of the isotope-coded propionylation procedure of Zhang et al. [Zhang et al., Rapid Commun. Mass Spectom. 16 (2002) 2325], which uses 'light' D0 and 'heavy' D10-propionic anhydride. The method has been extensively modified to improve both the kinetics and overall yield of propionylation. Using albumin as a model protein, the overall variation in quantification yields, calculated using several tryptic peptides, was within ±10% (S.D. ±0.2) error. The efficacy of the method is demonstrated by the quantitative differences obtained for vimentin in cell lysates of C2C12 myoblasts upon their myogensis to myotubules.

Keywords: Quantitative proteomics; N-terminal isotope tagging (NIT); Propionylation; nanoLC ESI/MS/MS; Myogenesis

1. Introduction

Western blot analysis is the most popular method to determine the level of a target protein in crude cell extracts. But in order to apply this method, the availability of specific antibodies directed to the target protein can be a critical limitation. In this situation, Western blot analysis for a novel protein must await the development of a highly specific antibody. Even in cases where there is an antibody suitable for Western blot analysis, it may not be suitable for quantification due to difficulties in optimizing the ratio of protein to antibody. While monoclonal antibodies are widely used for Western blot analysis, individual immunoglobulins may preferentially recognize a particular conformation of its target epitope [1–3].

Consequently, not all monoclonal antibodies are suitable for use as probes in Western blots, where the target proteins are thoroughly denatured. Polyclonal antisera, on the other hand, are undefined mixtures of individual immunoglobulins, whose specificity, affinity, and concentration are often unknown. As a result, it is not possible to predict the efficiency with which a given polyclonal antiserum will detect different antigenic epitope of an immobilized, denatured target protein [2,4]. Significant loss of proteins during the transfer to nitrocellulose filter is another problem [5]. Thus, an alternative technique to Western blot analysis that does not require an antibody to each protein has been needed, and recently more attention has given to substitute quantitative proteomics for Western blot [6].

Proteomics is the field of research studying all proteins expressed by the genes on a genome [7–13]. Mass spectrometry has emerged as a preferred tool for proteomics due to an attractive combination of sensitivity, specificity, and speed. Of particular importance is the high specificity that mass spectrometric approaches can afford while simultaneously providing widespread applicability. Reversed-phase nano-flow liquid chromatography (RP-nanoLC) combined with electrospray ionization tandem mass spectrometry (ESI MS/MS) is the prevailing technique for the analysis of peptides aimed at complete characterization of biological sample [14–18]. Much of this gain in sensitivity at the mass spectrometer is due to the combina-

* Corresponding author. Tel.: +82 2 2123 3448; fax: +82 2 392 3488.
E-mail address: yskim@yonsei.ac.kr (Y.S. Kim).

1570-0232/$ – see front matter © 2005 Elsevier B.V. All rights reserved.
doi:10.1016/j.jchromb.2005.07.039

tion of concentration dependent type ionization devices like ESI with on-line capillary separation devices of very small inside diameter.

Quantitative proteomics has been developed based on the use of isotope coded tagging. The use of stable isotopic nuclei (^{13}C, ^{15}N, D) in concert with MS for quantitative analyses is common in the field of small molecule research. Known amounts of isotope labeled versions of drugs or metabolites are spiked into a sample and compared with the unlabeled variant for the purpose of quantification. The similar concept for quantification of peptides has been greatly aided by the development of in vitro and in vivo isotope coding methods for peptides and proteins in complex mixtures [19–25]. Generally, the labeling methods of peptide and protein can be broadly classified into two groups based on incorporation of the quantitative tag: (1) metabolic labeling, where labeling is achieved by growing cells in media enriched in stable isotope-containing anabolites [26,27] and, (2) chemical incorporation, which relies on chemical modification of peptides in a site-specific manner after digestion of the proteins [28]. These labeling strategies depend on both sample species (tissue or cell) and targeting subject (specific-peptide or cell lysate). Chemical incorporation methods are more adaptable to diverse sample applications as well as the simplicity of MS/MS identifications [22,25,29–31]. For protein quantification by this chemical modification and mass spectrometry, isotope-coded affinity tags (ICAT) has been considered the most popular and well defined method [2,21,32,33]. However, ICAT is a time-consuming, expensive, multi-step approach and has critical limitations. Cysteine, which is the target amino acid residue for ICAT reagent is a relatively low abundant amino acid in proteins and post-translational modifications of cysteines make them less reactive to ICAT reagent. In these isotopically coded tagging, large tagging agents such as ICAT (442Da) can generate fragmented ion that may interfere with reverse-phase retention times, as well as MS/MS sequencing. If peptides are derivatized at two sites, their molecular weight will be increased by 884 amu, thereby generating more complex MS/MS spectra because ICAT derivatization could contribute 15–63% of the mass of derivatized peptides [34,35]. These cause the low peptide coverage of protein, indicating the risk to the representative of protein quantification. Mass coded affinity tagging (MCAT) is another method for the quantification of protein. In this method, lysine is chemically converted into homoarginine, which is 42 amu heavier than lysine. As a result, C-terminal lysine is the target for the quantification. But MCAT is limited in that the chemical reactivity of guanidination is not equivalent in all peptides [20].

Recently, Annan and co-workers investigated and validated a N-terminal isotope tagging (NIT) method using D_0/D_{10}-propionic anhydride [36,37]. This technique is rapid, sensitive, quantitative, and capable of identifying target protein out of extremely complex mixtures without bias or need for extensive purification of intact proteins. However, there are some difficulties with the NIT method, especially the kinetics and extent of propionylation and further optimization is warranted. In this paper, we describe a modified version of the NIT method and demonstrate its efficacy by quantitatively evaluating protein expression changes during myogenic differentiation of C2C12 cell.

2. Materials and methods

2.1. Materials

D_{10}-propionic anhydride (98%) was purchased from Cambridge Isotope Laboratories Inc. (Boston, MA, USA). Propionic anhydride (99%), urea, hydroxylamine, bovine serum albumin (BSA), ammonium hydroxide, ammonium bicarbonate, iodoacetamide, dithiothreitol (DTT), α-cyano-4-hydroxycinnamic acid and formic acid were purchased from Aldrich (St. Luis, MO, USA). Sequencing-grade modified trypsin was purchased from Promega (Madison, WI, USA). All water used in the experiments was purified by a Milli-Q system (Bedford, MA, USA). Methanol and acetonitrile (HPLC grade) were purchased from J.T. Baker (Phillipsburg, NJ, USA). Bradford protein assay kits were purchased from Bio-Rad (Hercules, CA, USA).

2.2. Cell lysis

The C2C12 cells (1×10^5 cells) were suspended in 200 μl of 25 mM ammonium bicarbonate containing 8 M urea and homogenized using Ultrasonic Processors (Ultraschallprozessor UP 200 s, Dr. hielscher, GER) for 30 s in the ice bath. The cell lysate was then centrifuged at 48,000 × *g* for 1 h at at 4 °C (Optima TLX ultracentrifuse, Beckman Instrumest Inc., Porterville, CA, USA). The supernatant was collected and the protein concentration was determined using the Bradford assay. The cell lysates (20 μg protein) were reduced by dithiothreitol (200 mM) and alkylated by iodoaceteamide (200 mM). Trypsin was added to the protein mixture (1:50, w/w trypsin-to-protein ratio) and the samples were digested overnight at 37 °C. Tryptic digest activity was quenched by adding 10 μl formic acid (10%). All samples for mass analysis were pre-treated with solid-phase extraction (SPE) [38].

Oasis HLB cartridge (Waters, Milford, MA, USA) and POROS R2 (Applied Biosystems, Framingham, MA, USA) were used for desalting and concentrating. Samples were loaded onto C18 columns and peptides were eluted with acetonitrile (50%) containing 0.1% formic acid. The elute was lyophilysed using the Centra VAC-802 (Vision, Incheon, KOR), and then re-dissolved in 100 μl distilled water.

2.3. D_0-, D_5-propionylation of peptides

The D_0- or D_{10}-propionic anhydride (10 μl) was added directly tryptic peptide mixtures (50 μl). The pH of the reaction mixture was maintained at pH 10 by the careful addition of ammonium hydroxide (30 μl). After the reaction at 60 °C for 1 h, hydroxylamine (1 M, 50 μl) was added to de-esterify any tyrosine residues. D_0- and D_5-propionylated tryptic peptides were mixed together and desalted by using SPE cartridges according to the manufacturer's protocols.

2.4. Nano-flow liquid chromatography

Ultimate NanoLC systems combined with FAMOS autosampler and Switchos column switching valve (LC-Packings, Amsterdam, The Netherlands) was used. First, samples were loaded onto pre-column (2 cm × 200 μm I.D.) (Zorbax 300SB-C18, 5 μm, Agilent, Palo alto, CA, USA) and washed with the loading solvent (H_2O/0.1% formic acid, flow rate: 4 μl/min) for 10 min to remove salts. And then, Switchos II column switching device transferred flow paths to analytical column (Zorbax 300SB-C18, 5 μm, 15 cm × 75 μm I.D.), the nano-flow eluted at a flow rate of 200 μl/min using a 110 min gradient elution from 0% solvent A to 32% solvent B, where solvent A was 0.1% formic acid with 5% actonitrile and solvent B was 0.1% formic acid with 90% acetonitrile. The column outlet was directly coupled to the high voltage ESI source, which was interfaced to the QSTAR Mass spectrometer [39].

2.5. ESI MS/MS analysis

MS/MS experiments were performed in parallel on a QSTAR Pulsar quadrupole TOF mass spectrometer (Applied Biosystems, Foster city, CA, USA), equipped with nano-electrospray ion sources (Protana, Odense, Denmark). The nanospray voltage was typically 2300 V in the nanoLC ESI MS/MS mode. The nanoLC ESI MS/MS running on QSTAR instrument were acquired in 'Information Dependent Acquisition' mode (IDA), which allows the user to acquire MS/MS spectra based on an inclusion mass list and dynamic assessment of relative ion intensity. The data acquisition time was set to 3 s per spectrum over *m*/*z* range of 400–1500 Da for nanoLC/MS/MS analyses.

2.6. MALDI-MS analysis

MAlDI-TOF MS was carried out on a Voyager-DE STR (Applied Biosystems, Forster City, CA, USA) equipped with VSL-337ND nitrogen laser of Thermo Laser Science. The acceleration voltage in the ion source was 20 kV with a grid voltage of 68% in reflector mode. The sample was mixed with a matrix of CHCA according to the instrument manual solutions (0.1% TFA, 50% acetonitrile solution).

2.7. Data search

Database searches were performed on an National Center for Biotechnology Information (NCBI) non-redundant database using the MASCOT software package (Matrix Sciences, London, UK). Especially, propionylated peptides were searched by modification parameter of propionyl-light (D_0) and propionyl-heavy (D_5). To remove overlapping peptides and low probability based Mowse scoring data, the search engine was set up predominant to bold-red matching results, establishing higher score than ion-search score. These identified proteins were classified with molecular functions, using Panther Classification System (http://panther.appliedbiosystems.com). For quantification procedure, acquisition software (Analyst QS, Applied Biosystems, Forster City, CA, USA) usually has tools for extracting single XIC (extracted ion chromatogram). The peak area represents the quantity of that peptide in the sample.

3. Results

3.1. Selection of unique tryptic peptides in BSA

In order to quantify a protein at the peptide level, unique peptides from the target protein must be selected. For example, BSA was in silico digested by trypsin to obtain 203 peptides (option: one mis-cleavage, carbamidomethylation, >500 Da). Of these 103 peptides were in the mass range 900–3500 Da. Of this subset of tryptic peptides, 30 peptides containing one Arg, two Arg (one in the middle mis-cleaved site and one at the end), one Arg in the middle and one Lys at the end, or one Lys at the end, were selected. Unique peptide selections improve the identification correlation score in peptide sequencing; reduce the misjudgment of protein expression. Those peptides containing Arg at the C-terminal end have good gas phase fragmentation [40]. The number of peptides that can be analyzed in nanoLC ESI MS/MS experiment depends on the chromatographic peak widths and the duty cycle of the instrument. With chromatographic peak widths of 10 s and scan times of 3 s per CID spectrum, three ions can be monitored with several spectra for each of the selected ions. BSA was digested by trypsin and analyzed by MS (nanoLC ESI MS/MS and MALDI TOF MS). The peptides detected reproducibly, were more than 14, but seven of them were unique. It is hard to predict any correlation between the sequence character and the intensity of mass spectrum at present but it depends probably on abundance of peptides and on the charged state of peptides.

3.2. Propionylation of peptides obtained from tryptic digestion of BSA

In order to ascertain whether each tryptic peptide is truly representative of BSA level, the tryptic digest was divided into two parts and labeled with D_0- or D_{10}-propionic anhydride in the presence of internal standard peptide. Propionylation with D_0- or D_{10}-propionic anhydride is similar to that for acetylation with acetic anhydride. D_{10}- refers to a molecule where the deuterium has been incorporated in place of the hydrogen. The N-terminal derivatization reaction of peptides by propionic anhydride is rather specific with some side reactions such as propionylation on epsilon amine of lysine and the hydroxyl group of tyrosine. The reaction depends on type of peptide, reaction temperature and time. The propionyl group on the hydroxyl group of tyrosine residue could be removed by the treatment with hydroxylamine but propionylation on epsilon amine of lysine residue could not be removed. Efforts to block this side reaction include guanidinylation of lysine [40,41]. Guanidination has favorable merits in peptide MS detection, but involve two chemical reaction steps, which depend on reaction pH, temperatures and time. Hence, decreased efficiencies in reactivity, sample recovery time occur.

In this study, no lysine epsilon amine blocking reactions were attempted. Unique target peptides were sorted into peptides containing none, or one Lys, mis-cleaved by trypsin.

Table 1
Propionylation reactivity of BSA peptides

Selected peptide	*m/z*	40 °C			60 °C		
		30 min	60 min	120 min	30 min	60 min	120 min
YLYEIAR (161–167)[a]	927.55	♦	♦	♦	♦	♦	♦
Pro[b]-YLYEIAR	983.55						
RHPEYAVSVLLR (360–371)	1439.37			♦		♦	♦
Pro-RHPEYAVSVLLR	1495.37						
LGEYGFQNALIVR (421–433)	1479.30		♦	♦		♦	♦
Pro-LGEYGFQNALIVR	1535.30						
DAFLGSFLYEYEYSR (347–359)	1567.17		♦	♦		♦	♦
Pro-DAFLGSFLYEYEYSR	1623.17						
MPCTEDYLSLILNR (469–482)	1724.09			♦	♦	♦	♦
Pro-MPCTEDYLSLILNR	1780.09						
RPCFSALTPDETYVPK (508–523)	1880.01	♦	♦	♦	♦	♦	♦
Pro-RPCFSALTPDETYVPK	1936.01						

Six BSA peptides were selected and monitored their reactivity on propionylation by MALDI TOF MS. ♦, indicates disappearance of peptide reactant in the reaction mixture.

[a] Site of amino acid sequence in BSA.

[b] Propionylated peptides.

These selected peptides were selected as candidates for MS/MS fragmentation. The effect of temperature and time on peptide propionylation was studied. Peptides YLYEIAR, MPCTEDYLSLILNR, and RPCFSALTPDETYVPK, were propionylated rapidly, whereas peptides RHPEYAVSVLLR, LGEYGFQNALIVR and DAFLGSFLYEYEYSR were rather slow at 60 °C. However, the reaction could be completed within 2 h at 40 °C or 1 h at 60 °C (Table 1). The propionylation was monitored by the disappearance of original peptide by using MALDI TOF MS. While MALDI TOF MS is not suitable for direct quantitative analysis, it is a useful tool for monitoring the behavior of reactants and propionylated-products.

3.3. Analysis for D_0- and D_5-propionylated peptides of BSA

D_0-and D_5-propionylated peptides of BSA were mixed together and analyzed by MALDI/TOF/MS. As shown in Fig. 1, the targeted six peptides were properly propionylated with the increase in molecular size 56 Da or 61 Da (56 + 5) in the presence of five deuterium. The *m/z* difference between deuteriated and non-deuteriated peptides was 5 Da for the peptides derivatized. The peptides doubly derivatized with propionyl group on N-terminal and epsilon amine, increased in molecular size 112 Da and 122 Da (112 + 10) with 10 Da differences to each peptide.

In order to quantify BSA using these peptides, nanoLC ESI MS/MS is useful since the selected peptides were directly sequenced by MS/MS to confirm their identity and were quantified by comparison of peak areas between deuteriated and non-deuteriated peptides in the ion chromatogram. To compare the ratio of deuteriated or non-deuteriated peptides, the peak area of the most abundant mono-isotope peak was selected. An internal standard peptide (Glu-fib: EGVNDNEEGFFSAR; 1569.67) was included in each sample. The relative ratios of peak areas for target peptides was calculated to compare with that of the peak for the internal standard peptide. After modification, the sample shows two dominant peaks in doubly charged forms in ESI ionization, one peak on 813.91 (*m/z*) [(1569.67 + 56.00 + 2)/2] with D_0-propionyl and another on 816.4 (*m/z*) [(1569.67 + 56 + 2 + 5)/2] with D_5-propionyl group, respectively. Triple charged peptide ions were excluded to avoid complication due to isotope peak overlapping. As shown in Table 2, eight peptides were classified into two groups; (1) Arg-

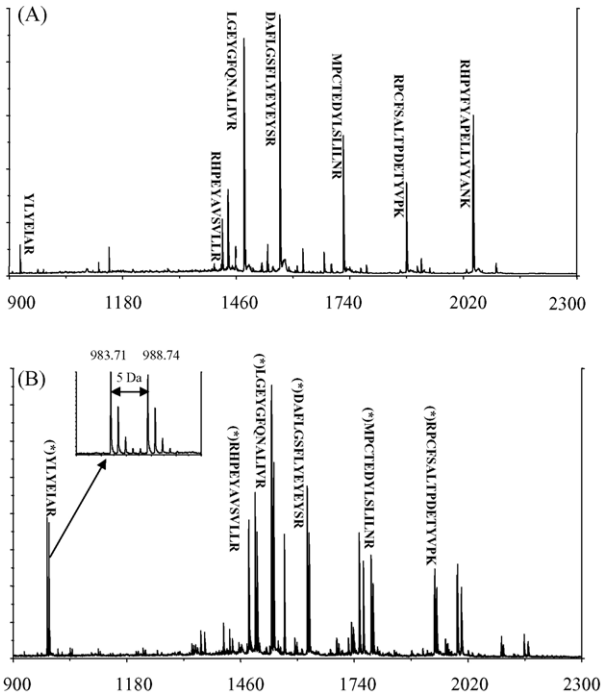

Fig. 1. MALDI-TOF mass spectra of peptides. (A) Mass spectrum of tryptic-digested BSA. The peptides indicated are unique, not homologours with other proteins. (B) Mass spectrum for mixture of D_0- and D_5-propionylated BSA peptides. Molecular masses are higher in 56 Da for D_0-propionylated and in 61 Da for D_5-propionylated peptide of BSA digests than in not propionylated peptides. (*) Indicates propionylation on N-terminal amine.

cleaved peptide which has no Lys in the peptide. (2) Peptides have one Lys on the C-terminal end or in the middle of peptide due to mis-cleavage. The First group peptides were good for this analysis. But the second group peptides made partially reacted forms. MALDI TOF MS spectra for the partially propionylated peptides were weak in comparison of that for the completely labeled peptide on N-terminal and epsilon amine of Lys, whereas RP nanoLC ESI MS/MS spectra were higher. It is because noise level was reduced due to chromatographic separation. As described above the complete reaction of all functional groups was not obtained but it was estimated that the identical results could be obtained under the same conditions. In Table 2, marked (*) peptides generated partially or completely labeled products. Selected peptides were screened on the bases of (1) double charged ions, (2) ions sequenced by MS/MS, (3) ions extracted precisely within two decimal places and (4) intensity analogous to internal-standard peptide. Using these guide lines, the peptides with reliable ratio could be extracted from many other labeling peptides. When the ratio of D_0- and D_5-propionylated peptides (1:1; 2:1; 3:1; 5:1; 10:1) was increased, the data obtained from experiments were well correlated to the ratio (Table 2). In order to perform this method successfully, application of a high resolution nanoLC ESI MS/MS analytical system is strongly recommended since chemical modification of peptides creates more complexity. To overcome this complexity, nano2D (SCX-RP)-LC MS/MS has been tried by many workers including us, but an optimum separation setting with higher sequence coverage is still required. In addition to these there is a point considered seriously. That is, deuteriated peptides behave reverse phase chromatographically different from that of non-deuteriated peptides. Generally, deuterium generates isotope effect in reverse-phase chromatography and affect on faster retention time and reduce mass peak resolution [35]. It has been suggested that this effect is low up to D_5-labeled peptide from the experiments with various units' deuteriated peptides. In this study this effect on D_5-propinylated peptide was determined by using the internal standard peptide (Glu-fib). After propionylation of EGVNDNEEGFFSAR (Glu-fib), 1569.67 Da, it showed two peaks in doubly charged forms, one peak on 813.91 (m/z) [(1569.67 + 56.00 + 2)/2] with D_0- and another on 816.4 (m/z) [(1569.67 + 56 + 2 + 5)/2] with D_5-propionyl group, respectively. Native Glu-fib generally eluted

Table 2
Relative peptide levels obtained from the selected BSA peptides

Selected peptides	Labeling	m/z	Relative abundance (D_0-pro-/D_5-pro-)				
			1:1	2:1	3:1	5:1	10: 1
RHPEYAVSVLLR	D0-pro-N-term	499.28	1.04	1.90	3.08	5.08	9.02
	D5-pro-N-term	501.78					
LGEYGFQNALIVR	D0-pro-N-term	768.90	1.10	2.12	3.08	5.05	11.21
	D5-pro-N-term	771.40					
MPCTEDYLSLILNR	D0-pro-N-term	890.93	1.11	1.81	2.71	5.10	10.90
	D5-pro-N-term	893.43					
RPCFSALTPDETYVPK[a]	D0-pro-N-term	968.98	0.99	1.88	3.04	4.95	11.40
	D5-pro-N-term	971.48					
	D0-pro-N-term;K	997.02	0.94	2.12	3.05	5.04	9.46
	D5-pro-N-term;K	1002.06					
TCVADESHAGCEK[a]	D0-pro-N-term	760.31	1.01	2.15	3.10	4.80	9.07
	D5-pro-N-term	762.81					
	D0-pro-N-term;K	788.32	1.12	2.14	3.01	4.85	9.61
	D5-pro-N-term;K	793.35					
LVNELTEFAK[a]	D0-pro-N-term	610.35	1.04	1.90	2.98	5.04	10.15
	D5-pro-N-term	612.85					
	D0-pro-N-term;K	638.50	1.18	1.95	3.00	5.15	11.01
	D5-pro-N-term;K	643.50					
K[a]VPQVSTPTLVEVSR	D0-pro-N-term	848.49	1.10	2.19	3.15	5.15	11.49
	D5-pro-N-term	850.99					
	D0-pro-N-term;K	876.52	1.14	2.16	3.02	5.20	9.24
	D5-pro-N-term;K	881.52					
HLVDEPQNLIK[a]	D0-pro-N-term	681.50	1.12	1.94	2.77	4.92	9.13
	D5-pro-N-term	684.00					
	D0-pro-N-term;K	709.40	1.14	2.11	2.93	4.89	8.88
	D5-pro-N-term;K	714.40					
Average ratio			1.08	2.03	2.99	5.02	10.04
S.D. (±)			0.07	0.13	0.13	0.13	1.01

Extracted ion chromatograms were obtained, each peak area of them was divided by that of internal standard peptide to normalize. The relative peak area's correlation were calculated by different levels of each labeled peptides.

[a] Indicates the another propionylation site at Lys(K).

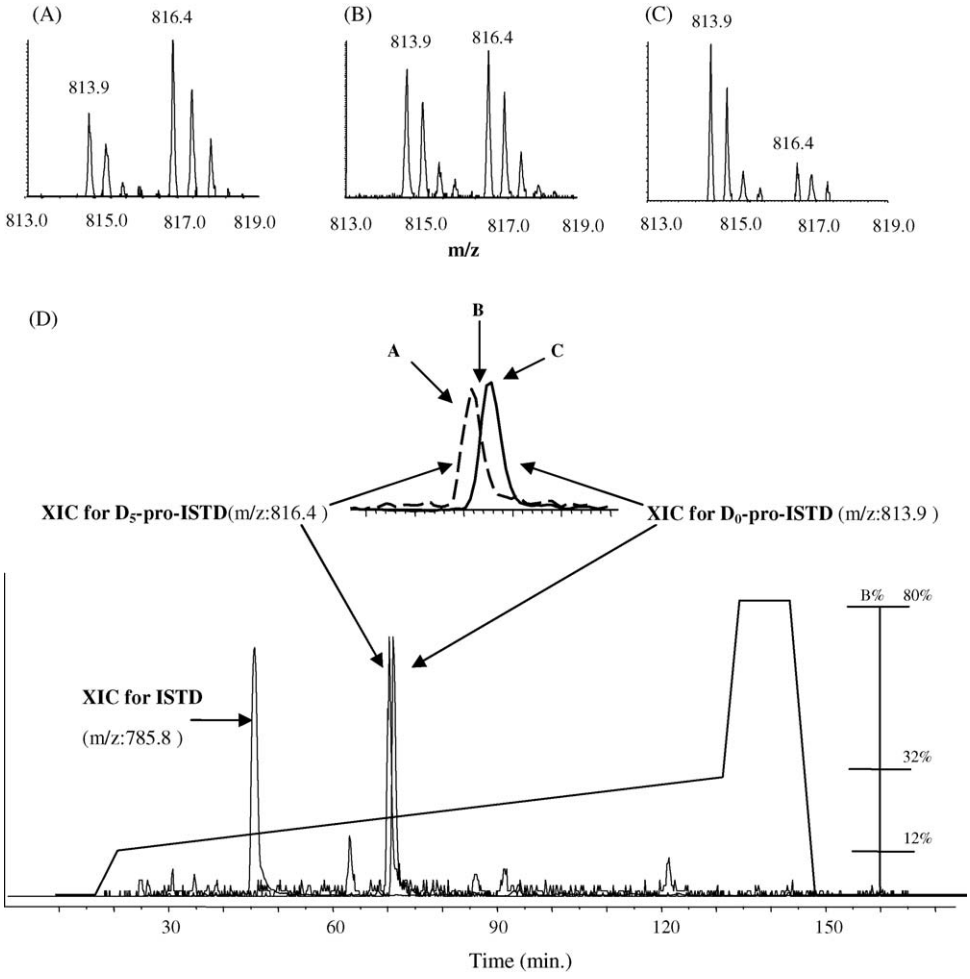

Fig. 2. Propionylation effect on reverse-phase ion chromatogram of standard peptide [Glu-fib EGVNDNEEGFFSAR, 1569.67 Da]. (A–C) Are mass spectra at different time point at (A–C) of extracted ion chromatogram (D). Standard peptide is eluted about 15% mobile phase (B). After propionylation, hydrophobic property of Glu-fib increase to 20% mobile phase (B). And then, which show the different retention time between D_0-pro-peptide [m/z 813.91 ≤ (1569.67 + 56 + 2)/2] and D_5-pro-peptide [m/z 816.4 ≤ (1569.67 + 56 + 2 + 5)/2] by isotope effects.

at 15% mobile phase B (0.1% formic acid, 90% acetonitrile) in reverse-phase chromatography. However, propionyl Glu-fib eluted at 20% mobile phase B with slight difference between deuteriated and non-deuteriated peptides (Fig. 2D). But the ratio of two peptides collected at different time points as shown in Fig. 2A–C, are very different. Therefore, in order to get a proper ratio of two peptides, it is important to compare a peak area on extracted ion chromatogram of a peptide with that of other peptide. All data in this study were obtained by the comparison of peak area. For the quantitative measurement, the selection of peak area of mono-isotope mass in extracted ion chromatogram (XIC) is practically ideal to avoid complexity due to isotope. And it is thought that the selection of 5 Da difference using propionyl group is better choice to minimize deuterium effect to retention time and to avoid peak overlapping in double charged ion. The propionylation of peptide gave also rather simple MS/MS spectra caused by alkyl-chain addition, compared with that obtained from ICAT, modified ICAT, or MCAT. Sequence analysis of propionyl peptides from fragmentation data was rather simple because in b-ion series additional 56 Da to peptide mass for non-deuterited proionyl peptides was monitored from b-1 ion to b-end-ion, whereas 61 Da for D_5-propionylated peptides was determined. On the other hand, in y-ion series sequencing from C-terminal end, there was no difference between deuteriated and non-deuteriated peptides (Fig. 3A and B). By this modified NIT method followed by nanoLC ESI MS/MS, the quantification of BSA was achieved successfully in about 10% error.

3.4. Proteome analysis in C2C12 myoblast and in myotube by using nano2D(SCX-RP) LC ESI MS/MS

The quantitative method described above was further evaluated by monitoring proteome changes during myogenesis, i.e., differentiating of C2C12 myoblasts to myotubes. Myoblast/myotube differentiation was effected by depletion of serum in the culture medium, as described previously [42]. After 4 days incubation, the cultured cells were tested to be myotube by microscopic observation and by the determination of change in the known marker proteins with Western blot

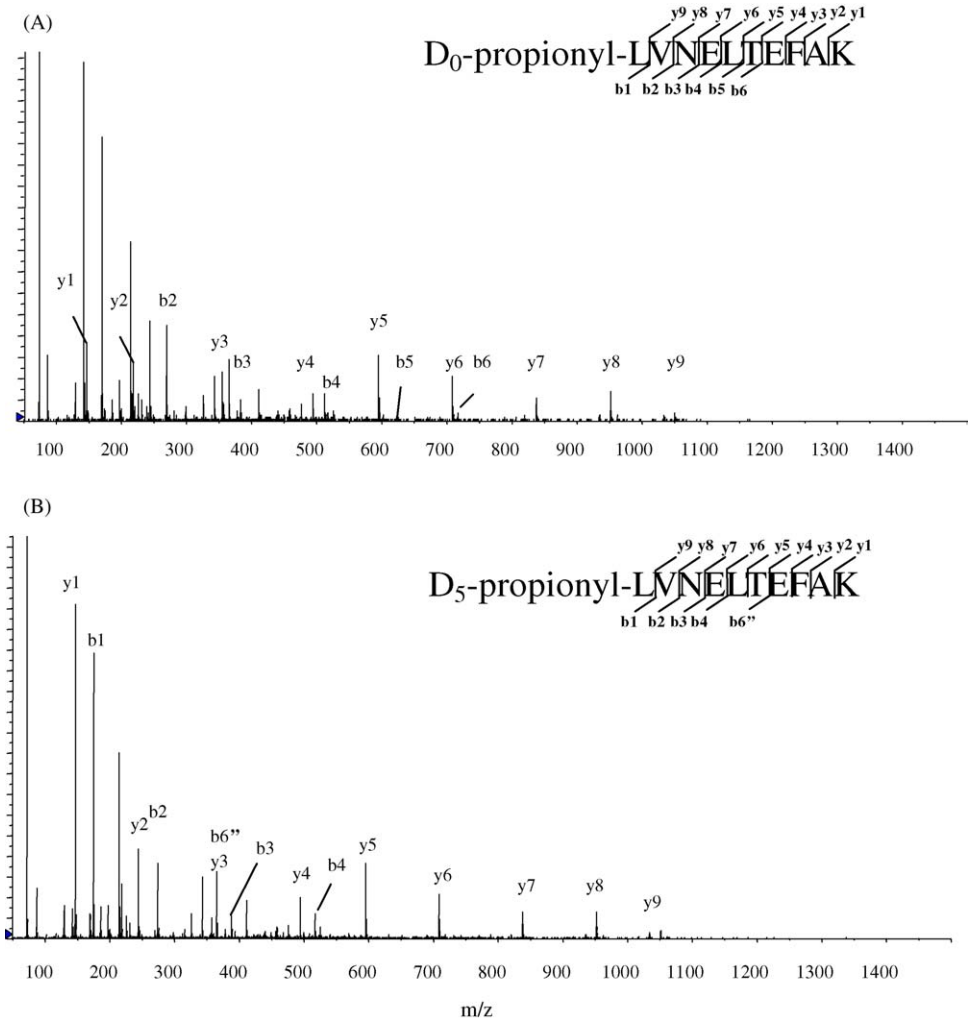

Fig. 3. MS/MS spectra of propionylated LVNELTEFAK. (A) D_0- and (B) D_5-propionylated peptide. Peptide sequencing was confirmed by Mascot peptide search data. b-ion series analysis is important for the comparison (Δ5 Da in mass) of modified peptides, whereas y-ion series data are essentially the same.

analysis (Fig. 5.) The proteins in myoblast and in myotube were identified using nano2D (SCX-RP)-LC MS/MS system without propionylation. By this method, about 1000 proteins from myoblast and myotube, respectively, were identified. However, after precise sorting with matching score of these data, 183 proteins in myoblast and 188 ones in myotube were filtered to be compared (Appendix A). Among them, 56 proteins including actin alpha-cardiac, glyceraldhyde-3-phosphate dehydrogenase, etc. were detected in both myoblast and myotube. This result suggested that 127 proteins including Arg/ser rich 14 splicing factor, non-metastatic protein (NM23A), galectin-3, etc. in myoblast are severely down-regulated during myogenic differentiation, whereas 132 proteins including archain1, bcl-2-interacting death suppressor, desmoyokin etc are highly up-regulated, perhaps induced (Fig. 4). However, the difference in the level of proteins detected in both myoblast and myotube could not be estimated. In order to determine the change in the protein level during myogenic differentiation, vimentin which was identified both in myoblast and myotube, this selected as a target protein [27,42].

3.5. Quantification of vimentin during myogenic differentiation

Cell lysates are very complex protein mixtures and, in general, it is very difficult to quantify a target protein in the mixture. However, the method described in this paper was successfully applied for this purpose. Vimentin has been known to be decreased during myogenesis [42] and in this experiment it was confirmed by 2-D SDS-PAGE and by Western blot (Fig. 5). In order to demonstrate the quantification of a protein in crude cell extract, vimentin was selected as a target protein. First, vimentin was in silico digested with trypsin resulting in ∼200 peptides including one mis-cleaved ones. Among them, 87 peptides were selected in the mass range, 750–3500 *m*/*z*. About half (43 peptides) of them were generated by Arg specific cleavage. However, only 20 peptides were unique, not homologous to other proteins; and these 20 were selected for further ESI MS/MS analysis.

Crude cell extracts, one from C2C12 myoblast and other from myotube, were prepared, taken equal amount of protein and

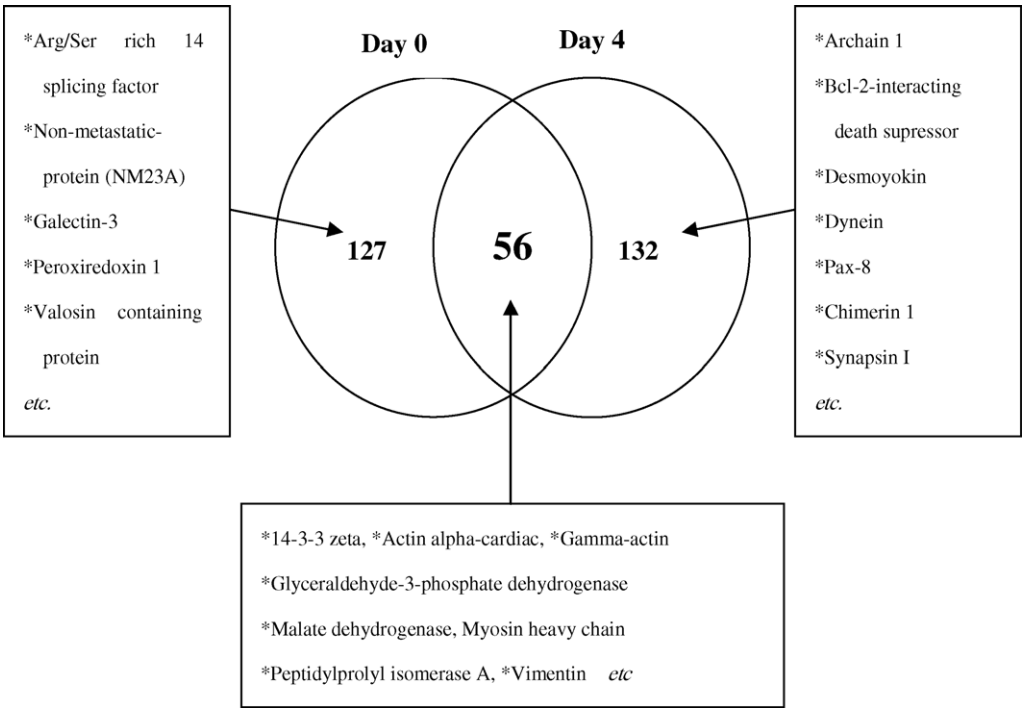

Fig. 4. Number of proteins identified in myoblast (Day 0) and myotube (Day 4) during myogenesis.

digested by trypsin, respectively. Then internal standard peptide (2 pmol/μl) was added to each sample. The peptides obtained from myoblast were propionylated by D_0-propionic anhydride, whereas those from myotube were done by D_{10}-propionic anhydride. These two samples were mixed, treated with hydroxylamine and analyzed by nanoRP LC ESI MS/MS. Fig. 6 shows the ion chromatogram generated by the combination of 12 extracted ion chromatograms for each selected peptides and internal standard peptides. Amino acid sequences of 28 peptides were confirmed by MS/MS analysis. As expected, two peaks for each peptide, one for proton coded and other for deuterium coded propionylated peptide (black peak), were obtained. The ratio of peak areas for the peptide were listed in Table 3, indicating that the ratios are well correlated in 0.61 ± 0.035 error range and that viementin was down regulated down to 60% during myogenesis. mRNA level determined by RT PCR was similarly down regulated, indicating that the expression of vimentin is transcriptionally regulated (data not shown). GAPDH was selected as a control protein for the analysis of vimentin since its level during myogenesis was known to be unchanged. GAPDH level was also confirmed by the data analysis (Fig. 6). In addition to these, the level of other proteins were also determined from the data analy-

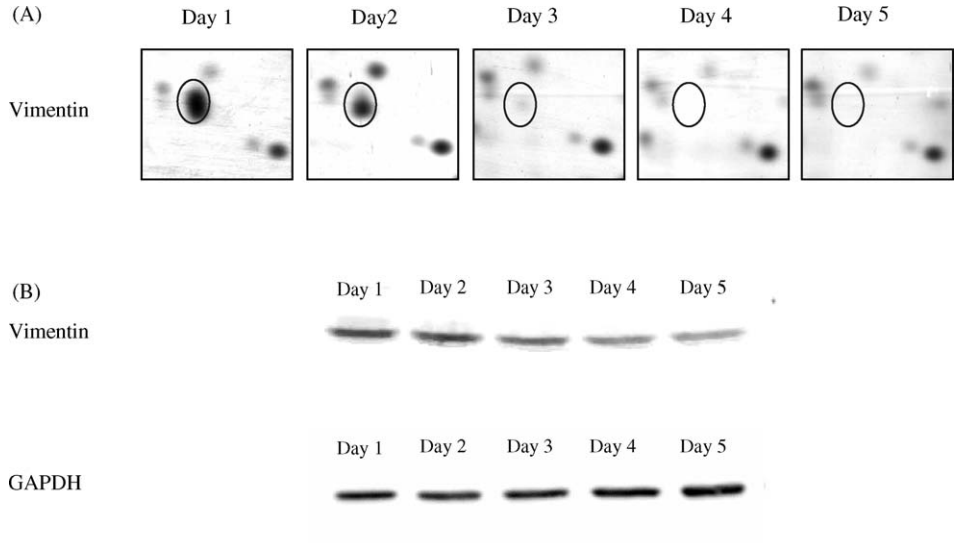

Fig. 5. Change of target protein level during myogenesis. (A) Vimentin spots on 2D SDS-PAGE gel and (B) Western blot analysis of vimentin and GAPDH.

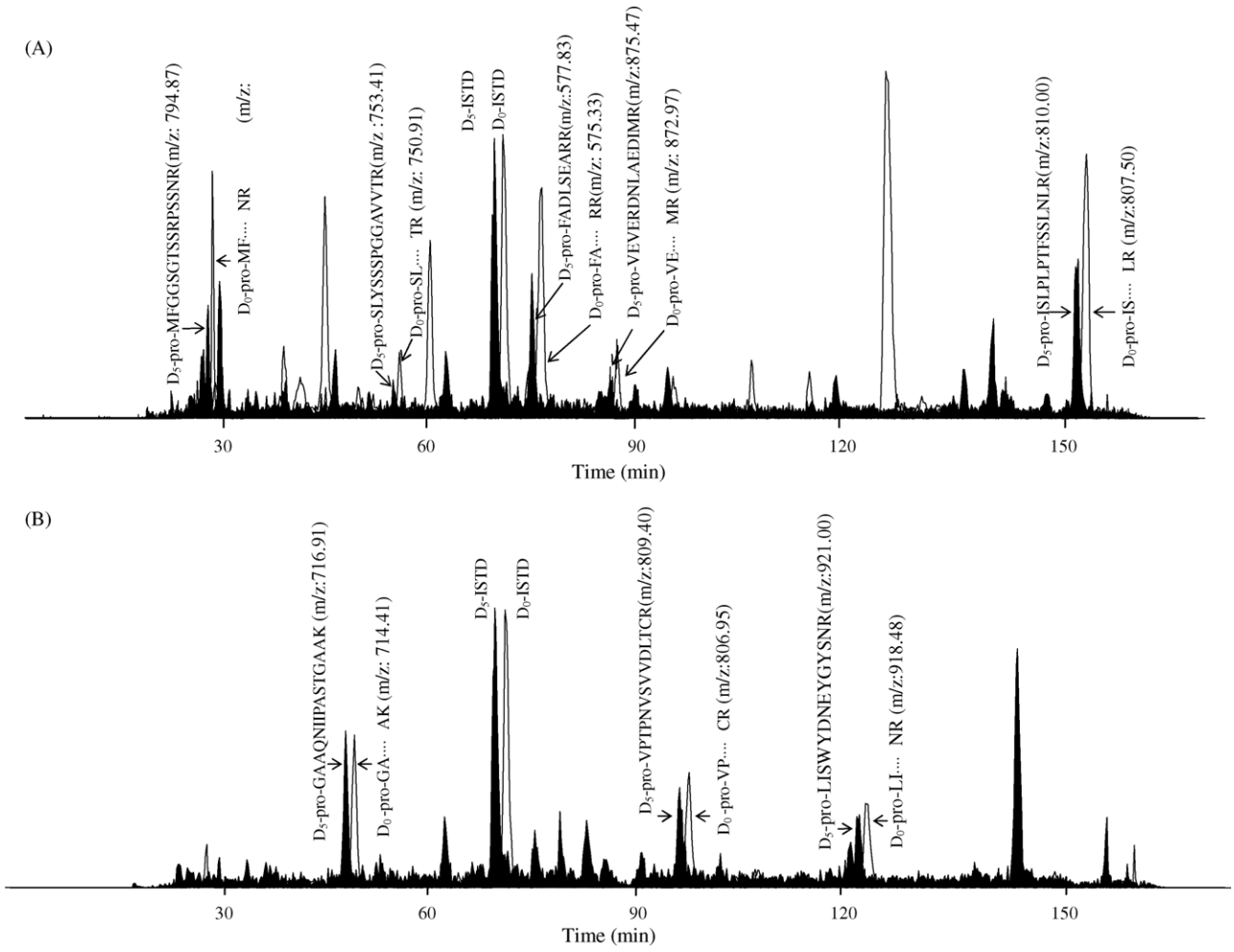

Fig. 6. Extracted ion chromatogram to quantify vimentin during myogenesis. (A) Vimentin; 10 different peptides (five D_0- and D_5-propionylated vimentin tryptic peptides) were scanned. (B) GAPDH, six different peptides (three D_0- and D_5-propionylated GAPDH tryptic peptides) were scanned. All spectral peak area was normalized by the comparison with those of the internal standard peptides. Selected peaks were confirmed by the analysis of MS/MS data.

sis: unchanged, gamma-actin (gi|809561) (1.06 ± 0.05), malate dehydrogenase (gi126897) (1.01 ± 0.04); up-regulated, actin alpha cardiac (gi|627834) (3.655), alpha enolase (gi|28485920) (1.33 ± 0.18), myosin heavyIX (gi|20137006) (1.37 ± 0.17), 14-3-3 zeta (gi|1841387) (1.490); down regulated, heat shock protein 1 (gi|6680305) (0.68 ± 0.10), elongation factor 1-alpha 1 (gi|1169475) (0.54 ± 0.07), peptidylprolyl isomerase A (gi|6679439) (0.84 ± 0.13), suggesting that many proteins are

Table 3
Relative abundance of proteins in myotube compare with C2C12 myoblast

Proteins	Score[a]	Protein level (myotube/myoblast)	Peptides (D_0- and D_5-)	Protein level
GAPDH (gi20820032)	405	1.105	Pro[b]-GAAQNIIPASTGAAK ;N-term	Unchanged
		1.094	Pro-VPTPNVSVVDLTCR ;N-term	
		1.046	Pro-LISWYDNEYGYSNR ;N-term	
		1.052	Pro-IVSNASCTTNCLAPLAK ;N-term	
		1.074 ± 0.029		
Vimentin (gi|281012)	657	0.595	Pro-FADLSEAANR ;N-term	Down regulated
		0.634	Pro-VEVERDNLAEDIMR ;N-term	
		0.556	Pro-MFGGSGTSSRPSSNR ;N-term	
		0.627	Pro-SLYSSSPGGAYVTR ;N-term	
		0.641	Pro-ISLPLPTFSSLNLR;N-term	
		0.611 ± 0.035		

[a] Indicate mascot protein identification score.
[b] Indicate propionylated peptides.

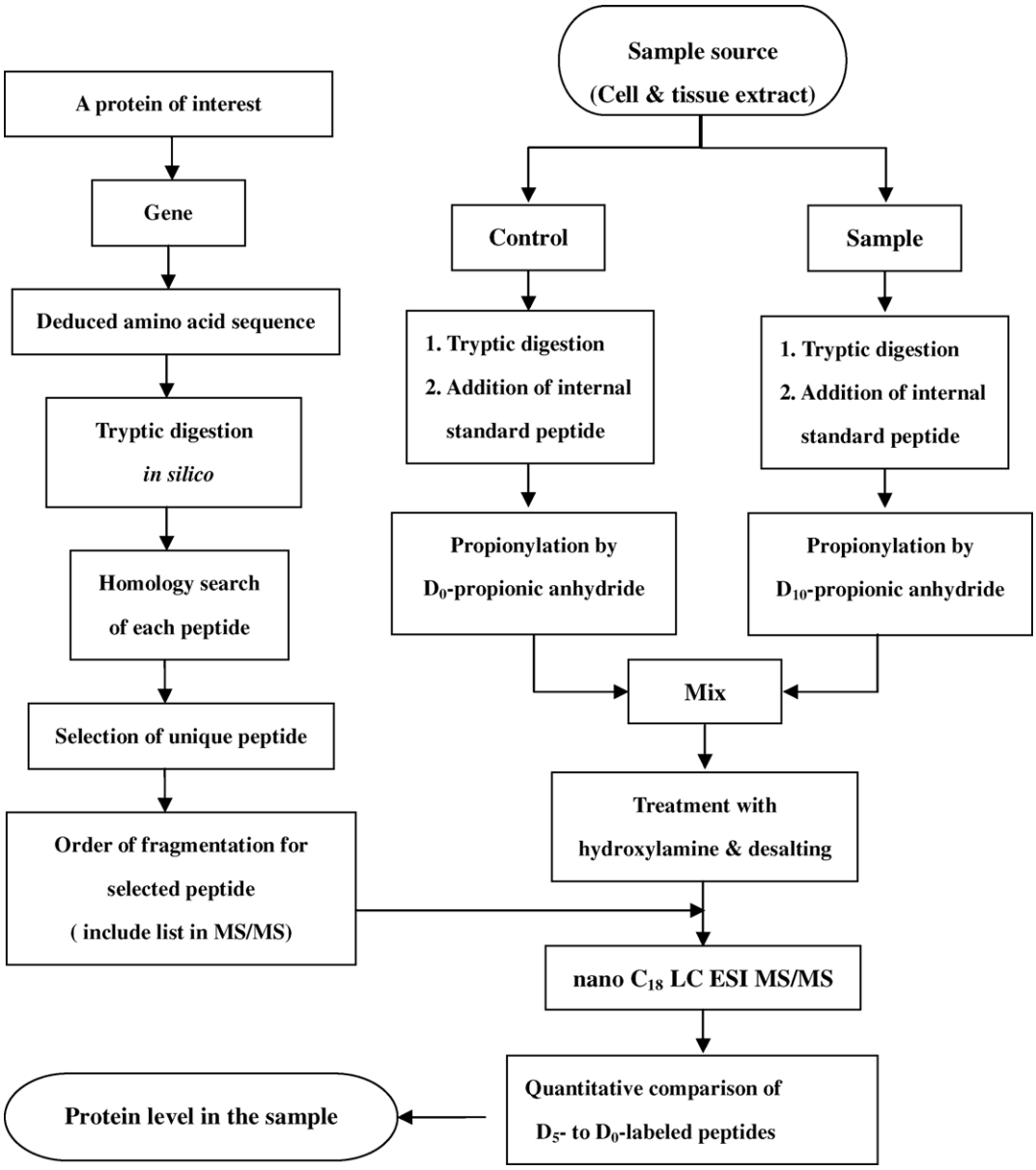

Fig. 7. A strategy for relative quantification of a protein of interest in sample.

up- or down regulated during myogensis. In 2D PAGE gel stained with Coomassie blue R 250 for the proteins in myotubes, one can hardly see vimentin, indicating that vimentin may not be exist in myotube. In a well developed Western blot picture, the level of vimentin was hard to estimate accurately. However, it could be determined accurately by the modified NIT followed by nanoLC ESI MS/MS that the level of vimentin in myotube was about 60% of that in myoblast.

4. Conclusion

Direct quantification of proteins in cell extracts is one of the major challenges in proteomics. Here we demonstrate that deuterium coded propionylation of tryptic peptides followed by high resolution nanoLC ESI MS/MS is a powerful tool for quantitative proteomics. Propionylation of tryptic peptides from a model protein (BSA) was successfully attained within 2 h at 60 °C. It is relatively cheap, rapid, and facile. Propionylation on hydroxyl group of Tyr could be removed by simple treatment with hydroxylamine. As shown in Fig. 7, a strategic approach is needed to get more accurate identification and quantification. Selection of proper peptide to be analyzed on mass spectrometry is important. Candidate tryptic peptides must be unique, i.e., not homologous with other proteins, and suitable for ionization in mass spectrometry (e.g., Arg-containing peptides [40]). Recently, mass spectrometric technologies in proteomics have greatly improved with proteins expressed in <15,000 cell copies in being determined by microLC ESI MS [6]. The combination of LC and mass spectrometry, especially nanoLC ESI MS/MS, now offers atto-mole level of protein detection [43].

In this study, we have used very successfully Qstar attached with nanoLC having 75 μm inner diameter (I.D.) capillary, 15 cm long, packed with C18 reverse phase resin, to routinely identify ∼1000 proteins from cell extracts. The number of proteins identified was even more when nano2D (SCX-RP)-LC in the modified capillary column was used. About 20% proteins among them could be filtered as ones with high score for identification. A salient feature of our present study was the observation that during myogenic differentiation, ∼127 myoblast proteins were significantly down regulated, whereas 132 proteins were newly appeared (up regulated) in myotubes. Of course, the functional validation of each of these proteins is required but it is very clear that the protein levels are high in myoblast and in myotube, respectively. These observations were readily be identified nanoLC ESI MS/MS alone, without having to perform Western blot analysis.

In summary, we describe here the relative quantification of cell extracts proteins. It is possible by using a combination of gene sequence data analysis to select unique peptides that are suitable for isotope coded propionylation to acquire their relative quantification by high resolution nanoLC ESI MS/MS. This method is able suitable for the quantification of any protein of interest in protein mixtures. The method is highly sensitive, selective, facile, and economical. It will be an even more powerful proteomic tool for quantitating low abundance proteins if used in conjunction with better methods of sample enrichment, pre-fractionation, affinity pull-down, etc. for target proteins of interest.

Acknowledgement

This work was supported by a grant (2003-2-0086) the Korea Science and Engineering Foundation through Protein Network Research Center at Yonsei University.

Appendix A. Appendix

See Table A.1.

Table A.1
Proteome analysis between myoblast (Day 0) and myotube (Day 4) during myogenesis

Molecular function	Protein	Day 0	Day 4	Score	GI
Cell adhesion molecule	Fibronectin 1 Fnl	0	0	383	28479106
	Vinculin (Metavinculin)		0	104	3287937
	CD 166 antigen precursor (Activated leukocyte-cell adhesion molecule)		0	42	5921181
Chaperone	47 kDa heat shock protein	0	0	155	303678
	Heat shock 70kD protein 8 Heat shock cognate protein 70	0	0	397	13242237
	Heat shock protein 1 (chaperonin 10) Hspel	0	0	77	6680309
	Heat shock protein HSP27	0	0	74	424145
	HSP60 protein (555 AA)	0	0	54	51452
	Similar to heat shock protein 84	0	0	242	27681923
	Tumor rejection antigen gp96 Tral	0	0	216	6755863
	Chaperonin subunit 6a (zeta) Cct6a	0		63	6753324
	Heat shock protein, A Hspa9a	0		112	6754256
	60 kDa heat shock protein, mitochondrial precursor (Hsp60)		0	54	3219998
	Chaperonin		0	64	460317
	dnaK-type molecular chaperone precursor, mitochondrial-mouse		0	54	1072476
	Heat shock protein, 1		0	319	29145077
Cytoskeletal protein	Myosin heavy chain IX Myh9	1	1.25	597	20137006
	Actin alpha, cardiac	1	3.27	280	627834
	Vimentin	1	0.6	819	2078001
	Lamin A [Mus musculus domesticus]	0	0	347	1794159
	Plectin isoform plec lb,2alpha	0	0	134	6578741
	Put. beta-actin (aa 27-375)	0	0	422	49868
	Trans gelin 2	0	0	120	9910901
	Tubulin alpha-2 chain (Alpha-tubulin 2)	0	0	430	135412
	profilin 1 Pfnl	0	0	101	6755040
	Actinin alpha 4 Actn4	0	0	232	11230802
	Calponin 3, acidic Cnn3	0	0	102	21312564
	FLJ00343 protein	0	0	312	28528531
	Desmin	0	0	684	20851164
	Dynein, axonemal, heavy chain 11 Dnahcll	0	0	112	6753652
	Alpha cardiac myosin heavy chain	0		131	191622
	Cardiac troponin T isoform Alb	0		47	1161066
	Filamin	0		42	9695286
	Myosin heavy chain IIB	0		67	9581821
	Periplakin	0		51	6851141

Table A.1 (*Continued*)

Molecular function	Protein	Day 0	Day 4	Score	GI
	Tropomyosin 2, fibroblast-rat	0		99	112442
	Tubulin, beta polypeptide	0		218	4507729
	Caldesmon 1 Caldl	0		45	21704156
	RIKEN cDNA 1110055E19 gene 1110055E19Rik	0		70	28522823
	Spectrin beta 2 Spnb2	0		87	7106421
	Tropomyosin 2, beta Tpm2	0		100	11875203
	Tubulin, alpha 4 Tuba4	0		249	6678467
	Actinin alpha 2		0	73	15149487
	Cytoskeletal beta-actin		0	93	3642631
	Microtubule-actin crosslinking factor 1 (actin cross-linking family 7)		0	123	14285343
	Myosin light chain alkali, smooth-muscle isoform (MLC3SM)		0	104	127148
	Skeletal muscle alpha-actin		0	280	387082
	Myosin XV Myol5		0	54	6754780
	Myosin, heavy polypeptide 7, cardiac muscle, beta Myh7		0	59	18859641
	Calponin 2 Cnn2		0	69	6680952
	Cofilin 1, non-muscle Cfll		0	218	6680924
	Formin Fmn		0	45	6806911
	Spectrin beta 1 Spnbl		0	46	7363453
	WD repeat domain 1 Wdrl		0	62	6755995
	Dystonin Dst		0	52	19882221
	Plectin 1 Plecl		0	83	20902637
	Kinesin family member 3A Kif3a		0	50	6680562
	Tumor protein, translationally-controlled 1 Tptl		0	50	6678437
	RIKEN cDNA A430056A10 gene A430056A10Rik		0	49	19527086
	Tubulin, beta 5 Tubb5		0	403	7106439
Extracellular matrix	Collagen type XXVII proalpha 1 chain	0		42	28204656
	Procollagen, type I, alpha 2 Colla2	0		92	6680980
	Collagen alpha 2(IV) chain precursor		0	52	115350
Hydrolase	Valosin-containing protein yeast Cdc48p homolog	0	0	214	6005942
	Chloride channel protein, skeletal muscle (Chloride channel protein 1)	0		54	13124069
	Polycystic kidney disease (polycystin) and REJ	0		43	6755086
	ATPase, Ca++ transporting, cardiac muscle, slow twitch 2 Atp2a2	0		128	6806903
	ATPase, ubiquitous sarcoendoplasmic reticulum Ca2+ ATPase		0	54	7949131
	Calcium channel, voltage-dependent, R type, alpha IE subunit Cacnale		0	80	25047158
	Sodium channel, voltage-gated, type V, alpha polypeptide Scn5a		0	51	14547893
Isomerase	Protein disulfide isomerase precursor (PDI)	0	0	215	129729
	Peptidylprolyl isomerase APpia	1	0.83	274	6679439
	Glucose regulated protein Grp58	0	0	146	6679687
	Peptidylprolyl isomerase (EC 5.2.1.8) CyP-Sl precursor	0		103	2118329
	Similar to peptidylprolyl isomerase A cyclophilin A (Interim) na	0		85	20843384
	Triosephosphate isomerase		0	108	1864018
	Similar to peptidylprolyl isomerase A cyclophilin A (Interim) na		0	73	25049082
Kinase	Myosin light chain kinase	0	0	96	14039490
	Mitogen activated protein kinase kinase kinase 11 mixed lineage kinase 3	0		71	11528494
	Mitogen-activated protein kinase 13 (Stress-activated protein kinase-4)	0		45	28381374
	Phosphatidylinositol 3-kinase, catalytic, alpha polypeptide Pik3ca	0		64	6679317
	Double cortin and calcium/calmodulin-dependent protein kinase-like 1	0		132	9910164
	Hexokinase		0	88	109966
	Pyruvate kinase, M2 isozyme		0	242	2506796
	Similar to Bmp2-inducible kinase		0	53	20829380
	Phosphoglycerate kinase 1 Pgkl		0	205	6679291
Ligase	Poly [ADP-ribose] polymerase-1 (PARP-1) (ADPRT)	0		48	130782
Lyase	Similar to Alpha enolase (2-phospho-D-glycerate hydro-lyase)	1	1.34	437	28485920
	Aconitase 2, mitochondrial Aco2	0	0	138	18079339
	Enolase 3, beta muscle Eno3		0	229	6679651
Membrane traffic	Ras-related protein Rab-7	0		79	1709999
Protein	Cytokine-dependent hematopoietic cell linker	0		40	7304965
	Electron transferring flavoprotein,	0		55	21704230

Table A.1 (*Continued*)

Molecular function	Protein	Day 0	Day 4	Score	GI
Molecular function	Unnamed protein product	0	0	327	12835845
Unclassified	Nestin Nes	0	0	145	15011851
	Ribosomal protein L27a	0	0	62	20842904
	Desmoyokin	0	0	178	109781
	Similar to Neuroblast differentiation associated protein AHNAK	0	0	175	20885364
	Unnamed protein product	0	0	60	26333513
	Unnamed protein product	0	0	86	26337133
	mKIAA1027 protein	0	0	112	28972572
	sox-4 protein	0		39	543326
	All-1 protein+GTE form (fragment)	0		66	627837
	Laminin alpha5	0		67	1586274
	BG	0		63	1675214
	Chain B, Crystal Structure Of The Nfkb P50P65	0		41	4139751
	Friedreich ataxia Frda	0		47	6679863
	gob-5 protein	0		54	7513665
	Teashirt 2	0		58	7578595
	Unnamed protein product	0		50	12842750
	Unnamed protein product	0		453	12844666
	Similar to KIAA0971 protein	0		50	14198427
	Tpr	0		44	14329713
	CCAAT displacement protein CDP	0		66	14346042
	WDR protein, form B	0		45	14970593
	Unknown (protein for MGC: 19001)	0		51	15636664
	Unknown (protein for IMAGE:4196534)	0		40	18490737
	Unknown (protein for MGC:37456)	0		86	19353593
	Unknown (protein for IMAGE:5035239)	0		43	19483918
	Putative coiled-coil protein	0		51	19526700
	Unknown (protein for IMAGE:5353935)	0		98	20380003
	Unknown (protein for IMAGE:4215522)	0		42	20810145
	RIKENcDNA5830411G16gene5830411G16Rik	0		64	20821617
	Similar to Hypothetical protein KIAA0514 (Interim) na	0		43	20823210
	Similar to hypothetical protein MGC19022 (Interim) na	0		44	20823579
	RIKEN cDNA 1700023E05 gene 1700023E05Rik	0		40	20834874
	Fibrous sheath-interacting protein 2 (Interim) LOC241516	0		55	20840764
	Hypothetical protein XP 157537	0		56	20879475
	Similar to CL2BB protein-rat (Interim) na	0		61	20879697
	RIKEN cDNA 4432416O06	0		44	20881204
	Hypothetical protein XP152805	0		40	20883542
	Similar to KIAA0712 gene product	0		45	20885248
	Hypothetical protein XP 156102	0		43	20893513
	RIKEN cDNA 1700034P14 gene 1700034P14Rik	0		46	20898018
	Similar to ATP-binding cassette, sub-family A member 3	0		49	20899064
	Similar to Bromodomain and PHD finger-containing protein 3	0		52	20899680
	Hypothetical protein XP 153455	0		44	20909946
	Hypothetical protein XP159560	0		51	20946708
	Similar to hypothetical protein MGC34831	0		59	20984588
	Unknown (protein for IMAGE:5325126)	0		48	21595152
	Similar to hypothetical protein FLJ20354	0		72	23271485
	RUN and FYVE domain-containing 2	0		53	23595371
	Similar to RIKEN cDNA 2410174K12 gene	0		39	24217436
	Similar to Retrovirus-related POL polyprotein	0		53	25020175
	Similar to KIAA0445 gene product	0		53	25031711
	Similar to a disintegrin-like and metalloprotease (reprolysin type)	0		41	25054191
	mKIAA0531 protein	0		51	26006171
	Unnamed protein product	0		59	26324998
	Unnamed protein product	0		40	26325794
	Unnamed protein product	0		175	26328693
	Unnamed protein product	0		70	26329513
	Unnamed protein product	0		60	26331358
	Unnamed protein product	0		97	26334227
	Unnamed protein product	0		59	26336156
	Unnamed protein product	0		50	26337747
	Unnamed protein product	0		40	26343623
	Unnamed protein product	0		71	26368624
	Unnamed protein product	0		50	26369191

Table A.1 (*Continued*)

Molecular function	Protein	Day 0	Day 4	Score	GI
	Gem (nuclear organelle) associated protein 5 Gemin5	0		39	27369782
	Transcriptional regulating protein 132 Trepl32-pending	0		53	27369896
	RIKEN cDNA 1700012H17 gene 1700012H17Rik	0		53	27734130
	Similar to synaptic SAPAP-interacting protein Synamon	0		45	28478605
	Similar to hypothetical protein FLJ10759 [Homo sapiens] (Interim) na	0		165	28481743
	Ubinuclein 1 Ubnl	0		52	28492802
	Calcyclin (AA 1-89)		0	58	49753
	Rev-Erb-beta		0	48	507211
	GDF5 protein		0	51	742374
	SEL1L		0	58	4159995
	KIF IB-beta		0	49	4512330
	Carnitine deficiency-associated protein expressed in ventricle 1		0	56	5921717
	Adenylyl cyclase-associated CAP protein homolog 1		0	173	6671666
	Telomerase associated protein 1 Tepl		0	42	6678285
	MYB binding protein (P160) la nuclear protein P160		0	85	7949086
	Unnamed protein product		0	44	12832665
	Unnamed protein product		0	104	12835827
	Unnamed protein product		0	52	12846287
	Unnamed protein product		0	69	12852148
	Unnamed protein product		0	47	12853735
	Unknown (protein for IMAGE:3483627)		0	152	13096866
	Unknown (protein for MGC:6299) [Mus musculus		0	41	16307569
	RIKEN cDNA 1300002P22 gene		0	43	16877282
	DEAD/H box polypeptide 36 protein		0	55	17863988
	CaV2.1		0	89	18958261
	Unknown (protein for MGC:36467)		0	51	20071690
	Golgi autoantigen, golgin subfamily a, 4 Golga4		0	63	20127150
	similar to MESOTHELIN PRECURSOR (CAK1ANTIGEN)		0	57	20844110
	Similar to CG10628 gene product		0	45	20862209
	Similar to NPD002 protein [Homo sapiens]		0	71	20865927
	Similar to filamin B, beta (actin binding protein 278) filamin B, beta		0	62	20869753
	Similar to hypothetical protein FLJ12547 [Homo sapiens] (Interim) na		0	42	20880396
	Hypothetical protein XP164746		0	44	20884305
	Similar to KIAA1858 protein [Homo sapiens]		0	60	20888575
	Similar to antigen LEC-A-mouse		0	48	20888669
	Similar to hypothetical protein [Homo sapiens]		0	65	20898146
	Similar to tubulin alpha 1		0	607	20903441
	Similar to Kinesin-like protein KIF14		0	49	20910649
	Similar to hypothetical protein MGC18735 (Interim) na		0	52	20945837
	Similar to Tho2 [Homo sapiens]		0	55	20983826
	RIKEN cDNA 4933437K13 gene 4933437K13Rik		0	49	21312778
	Similar to erythrocyte protein band 4.1-like 1		0	51	21961351
	T-complex protein 1, beta subunit (TCP-1-beta) (CCT-beta)		0	57	22654291
	Unknown (protein for IMAGE:4920887)		0	343	23272966
	RIKEN cDNA 3110065L21		0	45	25056266
	Unknown (protein for IMAGE:4235255)		0	46	26251716
	Unnamed protein product		0	62	26327461
	Unnamed protein product		0	52	26331384
	Unnamed protein product		0	88	26340122
	Unnamed protein product		0	345	26345590
	Unnamed protein product		0	47	26345686
	Unnamed protein product		0	68	26352740
	Unnamed protein product		0	227	26354418
	Unnamed protein product		0	45	26354977
	Similar to interferon gamma inducible protein 30		0	42	28525375
Nucleic acid binding	Eukaryotic translation elongation factor 1 beta 2	0	0	95	9055210
	H3.3 like histone MH321	0	0	64	484531
	Ribosomal protein S7 40S ribosomal protein S7 [Homo sapiens]	0	0	77	4506741
	Elongation factor 2 (EF-2)	0	0	303	18202285
	Histone protein Hist2h2ab	0	0	186	27372668
	H2A histone family, member X H2afx	0	0	144	7106331
	Similar to histone H2A, 1-mouse (Interim) na	0	0	201	20345628
	RIKEN cDNA 2610510L01 gene 2610510L0 IRik	0	0	46	13385520
	Ribosomal protein, large P2 Rplp2	0	0	174	13385524

Table A.1 (*Continued*)

Molecular function	Protein	Day 0	Day 4	Score	GI
	Histone H2A	0		120	631691
	H2A histone family, member Z H2AZ histone	0		64	4504255
	Similar to heterogeneous nuclear ribonucleoprotein A3 (hnRNP A3)	0		63	20879857
	Arnine/serine-rich 14 splicing factor	0		42	27370118
	Heterogeneous nuclear ribonucleoprotein U Hnrpu	0		51	7949051
	RIKEN cDNA 2010203J19 gene 2010203J19Rik	0		65	13385408
	Similar to 40S ribosomal protein S2 (Interim) na	0		43	28492318
	U5 small nuclear ribonucleoprotein Snrpl 16-pending	0		41	6755594
	Histone H2a(B)-613		0	164	1458139
	H4 histone family, member A [Homo sapiens]		0	251	4504301
	Ribosomal protein S28 40S ribosomal protein S28 [Homo sapiens]		0	43	4506715
	ELAV (embryonic lethal, abnormal vision, Drosophila)-like 1		0	43	6754262
	Zinc finger protein wizL-mouse		0	74	7513887
	Heterogeneous nuclear ribonucleoprotein K (hnRNP K)		0	75	12230552
	Similar to H2B histone family, member A		0	97	25052836
	DEAD/H (Asp-Glu-Ala-Asp/His) box polypeptide 39 Ddx39		0	58	20885603
	RIKEN cDNA 2400003003 gene 2400003O03Rik		0	71	20149756
	Heterogeneous nuclear ribonucleoprotein HI Hnrphl		0	56	10946928
	Diaphanous homolog 3 (Drosophila) Diap3		0	45	9789931
	Heterogeneous nuclear ribonucleoprotein A2/B1 Hnrpa2bl		0	135	7949053
	Ribosomal protein L10A RpllOa		0	41	6755350
	Ribosomal protein L6 Rpl6		0	121	6755354
	Ribosomal protein S3 Rps3		0	77	6755372
	Similar to ribosomal protein S20, cytosolic [validated]-rat (Interim) na		0	47	20875700
	Similar to ribosomal protein L7a, cytosolic [validated]-rat (Interim) na		0	61	28494316
Oxidoreductase	Malate dehydrogenase, mitochondrial precursor	1	1.01	193	126897
	glyceraldehyde-3-phosphate dehydrogenase Gapd	1	1.07	436	6679937
	Malate dehydrogenase, soluble	0		41	6678918
	Dihydrolipoamide dehydrogenase	0		59	6681189
	Similar to Glutamate dehydrogenase, mitochondrial precursor (GDH)	0		46	20843552
	Similar to glyceraldehyde-3-phosphate dehydrogenase (Interim) na	0		106	25020912
	Hydroxyacyl-coenzyme A dehydrogenase/3-ketoacyl-coenzyme A	0		104	20824845
	Diaphorase 1 (NADH) Dial	0		151	19745150
	Peroxiredoxin 2 (Thioredoxin peroxidase 1)		0	76	2499469
	Peroxiredoxin 4 Prdx4		0	65	7948999
	Lactate dehydrogenase 1, A chain Ldhl		0	173	6754524
	Similar to glyceraldehyde-3-phosphate dehydrogenase [Rattus norvegicus]		0	67	20878370
	Similar to glyceraldehyde-3-phosphate dehydrogenase [Sigmodon hispidus]		0	58	28526891
Phosphatase	Similar to testicular acid phosphatase precursor isoform a	0		55	20828437
Protease	Cathepsin B	0	0	93	227293
	Similar to protease (Interim) na	0		43	20888703
	RIKEN CDNAB230215L03 gene B230215L03Rik		0	52	23595060
	Small optic lobes homolog (Drosophila) Solh		0	47	7657601
Receptor	Nascent polypeptide-associated complex alpha polypeptide Naca	0	0	131	7305297
	ATP synthase, H+ transporting, mitochondrial Fl complex, alpha subunit	0	0	275	6680748
	Ephrin type-A receptor 2 precursor	0		67	1706570
	G protein-coupled receptor 56 serpentine receptor secretin receptor	0		37	9256531
	Similar to Antrax toxin receptor precursor (Tumor endothelial marker 8)	0		42	20873086
	Tissue-type vomeronasal neurons putative pheromone receptor V2R2	0		39	9910304
	RIKEN cDNA C030022K24 gene C030022K24Rik	0		43	22296591
	Low density lipoprotein receptor-related protein 1 Lrp 1	0		54	6678720
	Plexin Al Plxnal		0	79	6679389
	Plexin A2 Plxna2		0	45	20835802
Select calcium binding protein	Calmodulin	0		46	508526
	Calcium binding protein calcium binding protein, 140 kDa	0		58	12831229
	Myosin light chain, phosphorylatable, fast skeletal muscle Mylpf	0		79	7949078
	Calreticulin Cab-	0		124	6680836
	Similar to S100 calcium binding protein All—data source:MGD,		0	172	20842484
	Piccolo		0	50	27372317
	S100 calcium binding protein A10 (calpactin) S lOOalO		0	94	6677833

Table A.1 (*Continued*)

Molecular function	Protein	Day 0	Day 4	Score	GI
Select regulatory molecule	14-3-3 zeta	0	0	69	1526539
	Beta-galactoside binding protein	0		67	193442
	RIKEN CDNA4931426N11 gene 4931426NllRik	0		45	27369828
	ADP-ribosylation factor 4 Arf4	0		44	6680720
	JNK/SAPK-associated protein-1		0	49	6141549
	Ras-GTPase-activating protein SH3-domain binding protein G3bp-pending		0	46	7305075
	Guanosine diphosphate (GDP) dissociation inhibitor 3 Gdi3		0	46	6679987
	ADP-ribosylation factor 2 Arf2		0	74	6671571
	Tyrosine 3-monooxygenase activation protein		0	131	6756039
Signaling molecule	Guanine nucleotide binding protein (G protein),		0	57	5174447
	Paralemmin		0	47	12963501
	Pregnancy zone protein Pzp		0	44	6680608
	CD37 antigen Cd37		0	48	6680880
	Diaphanous homolog 1 (Drosophila) Diap 1		0	48	6681183
	A disintegrin-like and metalloprotease with thrombospondin type 1 motif		0	47	6752976
Synthase and synthetase	Citrate synthase Cs	0	0	53	13385942
	Phosphatidylserine synthase 2	0		64	7305419
	ATP synthase, H+ transporting mitochondrial Fl complex,	0		321	7949003
	Nitric oxide synthase 1, neuronal Nosl	0		54	6724321
	Tyros ine aminotransferase Tat	0		39	22122769
	Farnesyl diphosphate synthetase Fdps		0	53	19882207
Transcription factor	Nuclear receptor-binding SET-domain protein 1 Nsdl	0		61	6679138
	TATA box binding protein (Tbp)-associated factor, RNA polymerase I		0	51	10946814
Transfer/carrier proteins	Annexin A2 Anxa2	0	0	202	6996913
	Annexin I (Lipocortin I) (Calpactin II) (Chromobindin 9)	0	0	353	113945
	Annexin A5 Anxa5		0	144	6753060
	Annexin A3 Anxa3		0	93	7304887
	Annexin A6 annexin VI, p68 Annexin VI		0	166	7304891
Transferase	Ribophorin II Rpn2	0	0	118	9790203
	RIKEN cDNA 5430438D01 gene 5430438D01Rik	0	0	39	20876882
	Heterogeneous nuclear ribonucleoproteins methyltransferase-like 2		0	44	9790109
Transporter	Na^+ and H^+-coupled glutamine transporter		0	193	17390825
Viral protein	Similar to Retrovirus-related POL polyprotein		0	51	25024570

References

[1] H. Yamamoto, S. Bitoh, M. Torii, S. Fujimoto, J. Immunol. 130 (1983) 1038.
[2] W.F. Patton, J. Chromatogr. B Anal. Technol. Biomed. Life Sci. 771 (2002) 3.
[3] A.D. Hess, C.J. Thoburn, W. Chen, A.E. Bright, Transplantation 75 (2003) 1361.
[4] D.L. Doolan, J.C. Aguiar, W.R. Weiss, A. Sette, P.L. Felgner, D.P. Regis, P. Quinones-Casas, J.R. Yates 3rd, P.L. Blair, T.L. Richie, S.L. Hoffman, D.J. Carucci, J. Exp. Biol. 206 (2003) 3789.
[5] G. Jacobson, P. Karsnas, Electrophoresis 11 (1990) 46.
[6] D. Arnott, A. Kishiyama, E.A. Luis, S.G. Ludlum, J.C. Marsters Jr., J.T. Stults, Mol. Cell Proteomics 1 (2002) 148.
[7] M.J. MacCoss, J.R. Yates 3rd, Curr. Opin. Clin. Nutr. Metab. Care 4 (2001) 369.
[8] W.H. McDonald, J.R. Yates 3rd, Dis Markers 18 (2002) 99.
[9] W.H. McDonald, J.R. Yates 3rd, Traffic 1 (2000) 747.
[10] P.G. Righetti, A. Castagna, F. Antonucci, C. Piubelli, D. Cecconi, N. Campostrini, G. Zanusso, S. Monaco, Clin. Chem. Lab. Med. 41 (2003) 425.
[11] J. Yates 3rd, M. Snyder, Curr. Opin. Chem. Biol. 8 (2004) 1.
[12] J.R. Yates 3rd, Ann. Rev. Biophys. Biomol. Struct. 33 (2004) 297.
[13] W. Zhu, C.I. Reich, G.J. Olsen, C.S. Giometti, J.R. Yates 3rd, J. Proteome Res. 3 (2004) 538.
[14] B. Devreese, K.P. Janssen, F. Vanrobaeys, F. Van Herp, G.J. Martens, J. Van Beeumen, J. Chromatogr. A 976 (2002) 113.
[15] T. Kosaka, T. Yoneyama-Takazawa, K. Kubota, T. Matsuoka, I. Sato, T. Sasaki, Y. Tanaka, J. Mass Spectrom. 38 (2003) 1281.
[16] E. Nagele, M. Vollmer, P. Horth, J. Biomol. Tech. 15 (2004) 134.
[17] E. Varesio, S. Rudaz, K.H. Krause, J.L. Veuthey, J. Chromatogr. A 974 (2002) 135.
[18] M. Vollmer, E. Nagele, P. Horth, J. Biomol. Tech. 14 (2003) 128.
[19] P.A. Everley, J. Krijgsveld, B.R. Zetter, S.P. Gygi, Mol. Cell Proteomics 3 (2004) 729.
[20] S. Gu, S. Pan, E.M. Bradbury, X. Chen, J. Am. Soc. Mass Spectrom. 14 (2003) 1.
[21] D.K. Han, J. Eng, H. Zhou, R. Aebersold, Nat. Biotechnol. 19 (2001) 946.
[22] M. Heller, H. Mattou, C. Menzel, X. Yao, J. Am. Soc. Mass Spectrom. 14 (2003) 704.
[23] J.L. Hsu, S.Y. Huang, N.H. Chow, S.H. Chen, Anal. Chem. 75 (2003) 6843.
[24] S. Julka, F. Regnier, J. Proteome Res. 3 (2004) 350.
[25] W.A. Tao, R. Aebersold, Curr. Opin. Biotechnol. 14 (2003) 110.
[26] Y. Oda, T. Owa, T. Sato, B. Boucher, S. Daniels, H. Yamanaka, Y. Shinohara, A. Yokoi, J. Kuromitsu, T. Nagasu, Anal. Chem. 75 (2003) 2159.
[27] S.E. Ong, B. Blagoev, I. Kratchmarova, D.B. Kristensen, H. Steen, A. Pandey, M. Mann, Mol. Cell Proteomics 1 (2002) 376.

[28] S.E. Ong, L.J. Foster, M. Mann, Methods 29 (2003) 124.
[29] J.A. Ranish, E.C. Yi, D.M. Leslie, S.O. Purvine, D.R. Goodlett, J. Eng, R. Aebersold, Nat. Genet. 33 (2003) 349.
[30] P.G. Righetti, N. Campostrini, J. Pascali, M. Hamdan, H. Astner, Eur. J. Mass Spectrom. (Chichester Eng.) 10 (2004) 335.
[31] X. Yao, A. Freas, J. Ramirez, P.A. Demirev, C. Fenselau, Anal. Chem. 73 (2001) 2836.
[32] F. Schmidt, S. Donahoe, K. Hagens, J. Mattow, U.E. Schaible, S.H. Kaufmann, R. Aebersold, P.R. Jungblut, Mol. Cell Proteomics 3 (2004) 24.
[33] Y. Lu, P. Bottari, F. Turecek, R. Aebersold, M.H. Gelb, Anal. Chem. 76 (2004) 4104.
[34] R. Zhang, F.E. Regnier, J. Proteome Res. 1 (2002) 139.
[35] R. Zhang, C.S. Sioma, R.A. Thompson, L. Xiong, F.E. Regnier, Anal. Chem. 74 (2002) 3662.
[36] X. Zhang, Q.K. Jin, S.A. Carr, R.S. Annan, Rapid Commun. Mass Spectrom. 16 (2002) 2325.
[37] F. Zappacosta, R.S. Annan, Anal. Chem. 76 (2004) 6618.
[38] M.W. van Hout, C.M. Hofland, H.A. Niederlander, G.J. de Jong, Rapid Commun. Mass Spectrom. 14 (2000) 2103.
[39] H. Lee, E.C. Yi, B. Wen, T.P. Reily, L. Pohl, S. Nelson, R. Aebersold, D.R. Goodlett, J. Chromatogr. B Anal. Technol. Biomed. Life Sci. 803 (2004) 101.
[40] F.L. Brancia, M.E. Openshaw, S. Kumashiro, Rapid Commun. Mass Spectrom. 16 (2002) 2255.
[41] F.L. Brancia, A. Butt, R.J. Beynon, S.J. Hubbard, S.J. Gaskell, S.G. Oliver, Electrophoresis 22 (2001) 552.
[42] N.S. Tannu, V.K. Rao, R.M. Chaudhary, F. Giorgianni, A.E. Saeed, Y. Gao, R. Raghow, Mol. Cell Proteomics 3 (2004) 1065.
[43] A.R. Ivanov, L. Zang, B.L. Karger, Anal. Chem. 75 (2003) 5306.